Optical Mapping with a Precise Image Registration to Observe Late Phase 3 EAD

Ignacio Hernández
Facultad de medicina de la UASLP/Dept. of physiology, SLP, México
Email: ignacio.hernandezpo@gmail.com

Tatsuhiko Arafune
The University of Tokyo, Dept. of Bioengineering, School of Engineering, Tokyo, Japan
Email: arafune@bmpe.t.u-tokyo.ac.jp

Nitaro Shibata
Shinjuku Mitsui Building Clinic, Tokyo, Japan
Email: shibata@isk-smbc.org

Masatoshi Yamazaki and Haruo Honjo
Nagoya University, Research Institute for Environmental Medicine, Nagoya, Japan

Ichiro Sakuma
The University of Tokyo, Dept. of Precision Engineering, School of Engineering, Tokyo, Japan

Abstract—Newly mechanisms of abnormal automaticity named as "late phase 3 early after depolarization (EAD)" was suggested recently, but it was still not fully analyzed experimentally yet. The aim of this study was to analyze the focal activities of late phase 3 EAD and clarify ventricular fibrillation (VF) reinitiation mechanisms. Methods and Results On a pathological heart specimen, we dosed Isoproterenol and Nicorandil to isolated Langendorff-perfused rabbit heart. Membrane potential (V_m) and intracellular calcium (Ca_i^{2+}) measurements were conducted using a simultaneous dual optical mapping system with high spatial resolution and an accurate image registration. In this research we observed the V_m and Ca_i^{2+} wave-front propagation of postshock activity and reinitiated VF after strong electric shock against VF induced by burst pacing protocol. In addition, the location where the VF likely arises from late phase 3 EAD was identified. Conclusions Evidence of late phase 3 EAD were captured, and included: (1) focal point as origin of reinitiated VF on 2D mapping image was measured, (2) Ca_i^{2+} upstroke was faster than V_m depolarization at focal point.

Index Terms—optical mapping, arrhythmia, abnormal automaticity, calcium mapping, late phase 3 EAD

I. INTRODUCTION

If a tachyarrhythmia relies on a specific pathway or site of automaticity, this site can be ablated by radiofrequency (RF) energy, a low-voltage treatment applied through an electrode catheter, to destroy the tissue where the arrhythmia originates. Catheter ablation procedures commonly are used to treat against atrial fibrillation (AF) and ventricular tachycardia (VT).

For patients who are diagnosed with recurrent AF, a common procedure is the isolation of the pulmonary veins (PV). Due to the fact that AF frequently begins or is maintained by an arrhythmogenic site in the PV, this site can be isolated, with success rates of 80% or higher.
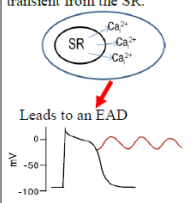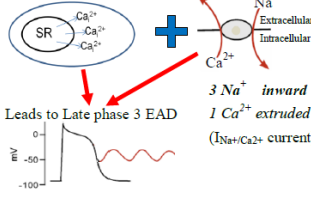
Catheter ablation can also be used for patients who are diagnosed with focal idiopathic VT/VF. Because this type of arrhythmia results from the right ventricular outflow tract (RVOT, 70%~80% of ventricular arrhythmias originate from this site), this site can be ablated, with success rates of more than 80% [1].

Several mechanisms have been postulated to underlie the initiation of AF and VT and the originated abnormal automaticity in atrial muscle sites, including abnormal automaticity, early and delayed after depolarization (EAD, DAD), as well as late phase 3 EAD [2]-[4]. Late phase 3 EAD has its own unique characteristics and represents a new concept of arrhythmogenesis in which abbreviated repolarization permits normal SR calcium release to induce an EAD-mediated closely coupled triggered response, particularly under conditions permitting intracellular calcium loading [5]. Table I shows the differences in EAD and late phase 3 EAD.

The ionic mechanism responsible for abnormal automaticity has not been conclusively explained, but may be attributed to a decrease in the outward potassium (IK1) and inward Ca^{2+} currents [6]. It has also been suggested that the release of Ca^{2+} from the sarcoplasmic reticulum (SR) may activate the Na^+/Ca^{2+} exchanger current, leading to spontaneous depolarization and abnormal automaticity [7]. A similar mechanism is

responsible for generating the DAD, EAD and recent studies have uncovered a novel mechanism that induces triggered activity, and has been termed "late-phase 3 EAD," which combines the properties of both EAD and DAD, but has its own unique characteristics [5].

TABLE I.   COMPARISON CONVENTIONAL EAD AND LATE PHASE 3 EAD

EAD	Late phase 3 EAD	
After resetting through DC shock or by rapid pacing (burst pacing)		
a) There is spontaneous overload of the Ca_i^{2+} transient from the SR.	a) Normal release of Ca_i^{2+} transient from SR.	b) Mediated by Na^+/Ca^{2+} exchanger
Leads to an EAD	Leads to Late phase 3 EAD	$3\,Na^+$ inward $1\,Ca^{2+}$ extruded ($I_{Na+/Ca2+}$ current)
1. Spontaneous calcium overload.	1. Short APD	
	2. Ca_i from the SR is insufficient for depolarization	
	3. Na/Ca exchange proceeds rapidly.	
	4. I_{Na} leads to new depolarization	
Trigger by	Overload of Ca_i^{2+}	I_{Na}
AP phase	Early phase of action potential	Phase 3

It has been thought that abnormal intracellular Ca^{2+} handling in cardiac tissue plays an important role in heart failure (HF). It was recently reported that the late phase 3 EAD caused by a shortened action potential duration (APD) and increased Ca^{2+} transient was the origin of abnormal oscillation after depolarization.

However, full understanding of the role of postshock activity after electric shock during VF remains unclear. Late phase 3 EAD occurs under different experimental conditions and depends on the mode of EAD induction, tissue/cell type used, drug used and experimental target. A common characteristic of late phase 3 EAD is that it is found under high calcium concentrations and short APD conditions. This novel mechanism is considered to play an important role in the initiation of several cardiac arrhythmias.

Previous studies as experimental measurement of late phase 3 EAD were reported by Chua *et al.* [8] based on a clinical condition called electrical storm, in which spontaneous ventricular fibrillation (SVF) requiring several defibrillation shocks occurs in patients with HF. Using normal and HF rabbit models, they investigated whether the apamin-sensitive potassium current (IKAS), which is increased in HF rabbit ventricular myocytes, was responsible for postshock APD shortening. They used apamin, a drug that blocks SK channels, in order to block IKAS to avoid APD shortening and recurrent SVF in HF ventricles. In addition, they suggested that excessive APD shortening might be related to the development of late phase 3 EAD.

However, the previous late phase 3 EAD research has various limitations, because the late phase 3 EAD phenomenon is difficult to induce, and also difficult to identify the reinitiating VF excitation propagation as late phase 3 EAD. Waveforms at the starting timing of late phase 3 EAD or V_m/Ca_i^{2+} mismatch 2D excitation propagation image has been reported, but the focal excitation propagation which is potent evidence of late phase 3 EAD had not been observed yet. One reason might be that their optical mapping system (at 2ms per frame and 100×100 pixels, spatial resolution of 0.35mm $\times$0.35mm per pixel) has limitations with regard to observing in detail the excitation of the heart.

In light of these limitations, to measure the V_m/Ca_i^{2+} relating phenomenon precisely, the postshock activities after strong electric shock against VF were assessed in a pathological model comprising an isolated rabbit heart specimen using the simultaneous V_m and Ca_i^{2+} mapping system with high spatial resolution and an accurate registration (at 250fps, pixel resolution is 512×512 pixel, spatial resolution is 0.09mm$\times$0.09mm per pixel) [9].

The objective of this study is to analyze, clarify the focal activities of late phase 3 EAD and confirm the transition mechanisms late phase 3 EAD to VF reinitiation.

II.   METHOD

A.   *Precise V_m/Ca_i^{2+} Optical Mapping System*

The optical mapping system used has been described in detail previously [9]. Briefly, main components of the optical system are two high speed CMOS digital cameras (Fastcam-Max, Photron, Tokyo, Japan), with the following specifications: temporal resolution=250fps, pixel resolution is 512×512 pixel, spatial resolution is 0.09mm$\times$0.09mm per pixel, grayscale 10 bits respectively. An excitation filter (λ=570nm) and LED ring light was used as excitation light source (195 LEDs, λ=525nm), for illuminating the epicardial surface of the heart. The fluorescent from the stained heart was passed through a dichroic mirror (45 degree color filter) to split the emission wavelength around below and above 630nm. Wavelengths below 645nm were passed through an interference filter (band pass filter, λ=580nm, FWHM=20nm) for Ca_i^{2+} signal and those above through a long pass filter (λ=700nm) for V_m signal and collected by each camera lens. Optical mapping system is shown in Fig. 1.
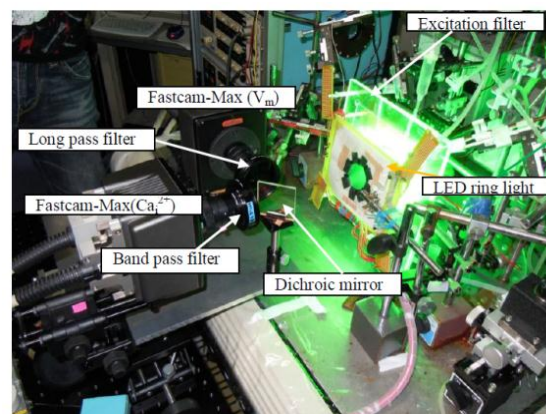

Figure 1.   System overview

B.   *Heart Specimen Preparation*

The protocol was approved by the Institutional Animal Care and Use Committee at Nagoya University. Langendorff-perfusion rabbit heart specimen was set up (hearts n=4). All hearts were loaded with the calcium-sensitive dye Rhod2-AM and the voltage-sensitive dye RH237. In addition, excitation-contraction uncoupler Cytochalasin D was added to the perfusate to eliminate motion artifact [10].

In order to perform late phase 3 EAD experiments, a specific experimental configuration was used, which was almost the same as was previously reported [9], apart from one aspect. Because late phase 3 EAD is difficult to induce and generally occurs in the atrium, to recreate the abnormal automaticity, two ion channel blockers were used to treat isolated Langendorff perfused rabbit hearts to simulate heart failure. Nicorandil (0.3mM/L) was used to enhance the short APD. It opens triphosphate-sensitive potassium (KATP) channels in the cardiovascular system and causes shortening of the APD. Isoproterenol (0.3μM/L) was used to increase the Ca^{2+} transient.

C. Experimental Protocol

In order to induce late phase 3 EAD during experiments, firstly VF was induced, then an electric shock against VF was applied, and finally, the postshock activity was recorded. During the experiments, the heart was continuously paced using rapid protocol pacing (burst pacing) selected in the range of S1-S1 which started from 600ms to 160ms decreased intervals, by 20 or 30 train pulses according to the previous interval selected. Then, we recorded the resulting phenomena (postshock activity). If VF occurred during this activity, an electric shock between 10V-100V was applied. Data was acquired for a total of 1200-1500 frames, around 100-200 frames before shock and approximately 1300 frames after the shock continuously. Total number of delivering electric shock was 20.

D. Software Processing

In order to achieve simultaneous measurement of two dynamic parameters from the same part of the heart surface, we developed image registration software. The registration algorithm was consisted by 2 steps. The first step was point based registration with the images of chess-board for calibrations. Then the second process was spatial transformation from point laser marker images and optimization with Mutual Information registration [9]. By this image registration, the accuracy of the registration was RMSE=0.57±0.36 pixel.

No processing was done on the signals other than to perform a spatial average in a 5×5 pixel area (0.5mm×0.5mm, the overall recording area after spatial averaging was therefore estimated to be 0.48mm^2) selected from the anterior surface of the heart to obtain both signals, and the baseline drift (if present) was removed.

III. RESULTS

A. Defibrillation Results

The following 3 groups were found through examination of all of the experimental data.

VF continued without change. After electric shock, the VF continued without change, and the postshock activity was not present (episodes n=12). Fig. 2 shows a typical example.

VF termination. After electric shock, the VF was successfully stopped. Postshock activity (the waveforms was like normal pacing activation) occurred once, and the cardiac electrical activation terminated (episodes n=7). Fig. 3 shows a typical example.

Late phase 3 EAD like phenomena. After electric shock, postshock activity occurred, and the VF reinitiated. (This episode was considered relevant to late phase 3 EAD, (episode n=1)). Fig. 4 illustrates this result. Among these three types of results, pattern 3 was considered to be relevant to late phase 3 EAD. Therefore, a detailed analysis was conducted on these data, which showed the following features characterizing late phase 3 EAD: 1. After the 1st postshock activity, there was a large Ca^{2+} transient and short APD. 2. New VF activity occurred at the end of the large Ca^{2+} transient 3. The Ca^{2+} transient occurred prior to the upstroke of Vm. One episode was selected as an episode satisfying the above three criteria characterizing late phase 3 EAD. The postshock analysis demonstrated that, from the optical map of V_m and Ca_i^{2+}, it was possible to identify the postshock activity (1, 2) and VF episode (3), and it was also possible to observe the excitement propagation in the whole heart.

B. Optical Mapping Analysis of Postshock Activity

1st. postshock activity. The 1st postshock activity is shown in Fig. 5, and is characterized by the following features: (a) an activation wavefront propagated from the apex to the base of the ventricles. V_m and Ca_i^{2+} changes started at the same time after the shock. (b) A large Ca^{2+} transient was present that progressively increased. In the snapshot of the optical mapping at frame No. 139 shows that the Ca_i^{2+} remained elevated throughout the mapped field, whereas the V_m began to repolarize near the apex.

2nd postshock activity. The 2nd postshock activity is shown in Fig. 6. Because of the large Ca^{2+} transient observed during the 1st postshock activity, the Ca_i^{2+} during the 2nd postshock activity remained elevated in the base area of the heart at the beginning of the 2nd postshock activity. A distinct Ca_i^{2+} wave was not observed from the apex to the base. On the contrary, the V_m propagated from the apex to the base of the heart. Fig. 4 shows the tracing of the V_m and Ca_i^{2+} at the observation point (2n-pink shaded region) shown in Fig 6. It shows a mismatch of the changes in the V_m and Ca_i^{2+}.

VF reinitiation episode. The 3rd postshock activity is shown in Fig. 7. The VF restarted from the 3rd postshock activity. We concluded that a new activation appeared from the location marked by the red dot in the image at frame No 180. The changes in the V_m and Ca_i^{2+} during the resultant VF were similar to those found in VF before shock application.

In addition, the large Ca^{2+} transient and short APD observed in the previous activities (the 1st and the 2nd postshock activities) were observed. This implies that the 3rd postshock activity could be caused by late phase 3 EAD.
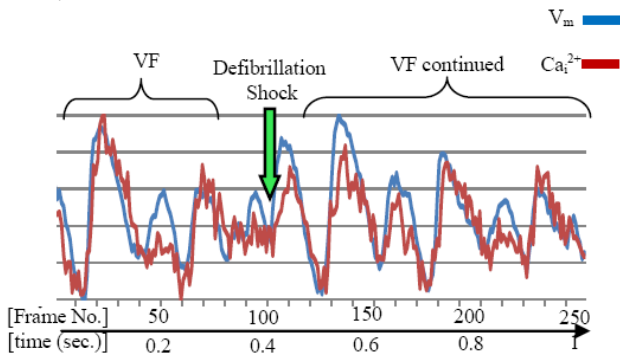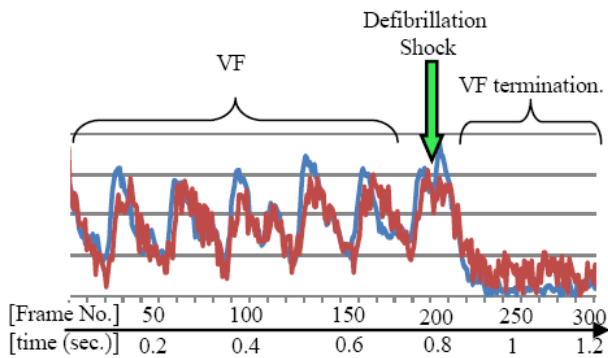

Figure 2. VF continued without change
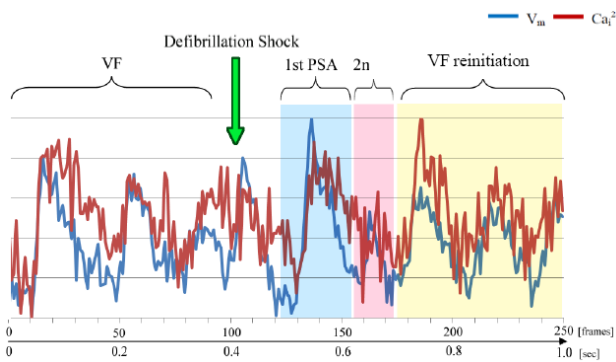

Figure 3. VF termination

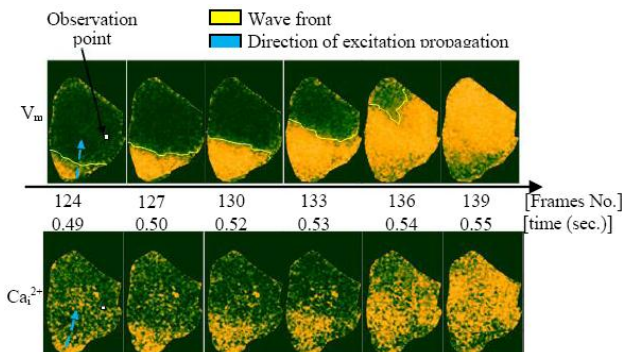Figure 4. Episode related to late phase 3 EAD

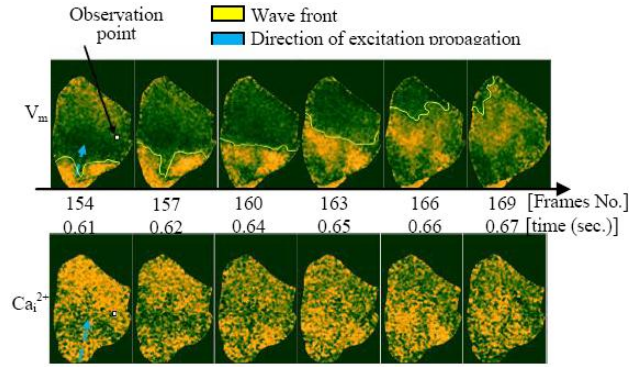Figure 5. Vm/Cai^{2+} optical mapping results of 1stpostshock activity

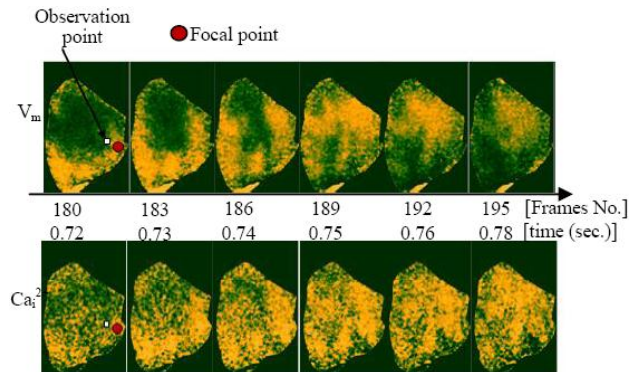Figure 6. Vm/Cai^{2+} optical mapping results of 2nd. postshock activity

Figure 7. Vm/Cai^{2+} optical mapping results of restarting VF and focal excitation propagation.

C. Confirmation of Late Phase 3 EAD

The propagation of the depolarized area and elevated calcium area, respectively, for the image frames 174 to 179 during the 3rd postshock activity implied that the elevated calcium region expanded earlier than the depolarized area.

The procedure used to calculate the area of interest (depolarized area and the elevated calcium area) for the V_m and Ca_i^{2+} optical image frames from 174 to 179 during the 3rd postshock activity was as follows:

First, the region of interest (ROI) was selected so that ROI included the area where the focal point started. The rest of the image was removed. Then, the image was binarized by setting the threshold at half of the amplitude of the V_m and Ca_i^{2+} signals in the previous beat. Fig. 8 shows an example of the procedure used.

To confirm the activation propagation is the focal activity, we calculated the number of pixel insides of the extracted depolarized area/elevated calcium area in the binary image.

The results of extracting depolarized areas and the elevated calcium areas for V_m and Ca_i^{2+} optical images frames from 174 to 179 are displayed in Fig. 9. It shows the propagation of the depolarized area and elevated calcium area, respectively, for the image frames 174 to 179 during the 3rd postshock activity. The data implied that the elevated calcium region expanded earlier than the depolarized area.

In Fig. 10, interestingly, the Ca_i^{2+} area monotonically increased, while the depolarized area immediately decreased and then began to increase at frame 176. This

indicates that the elevation of the Ca_i^{2+} in this region could occur earlier than depolarization, suggesting that the phenomenon occurring in this region could be attributed to late phase 3 EAD.
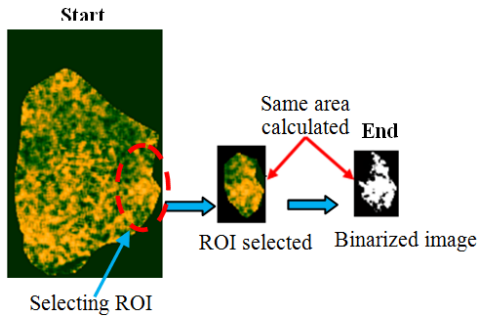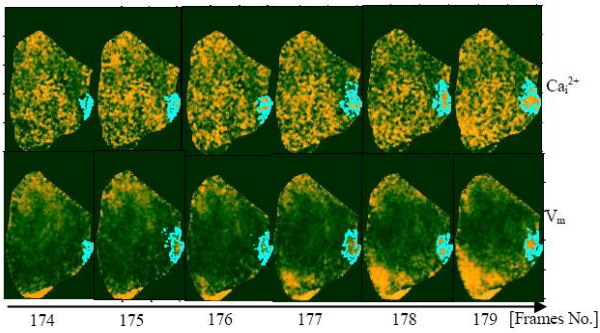

Figure 8.   Alculation procedure of area interest.

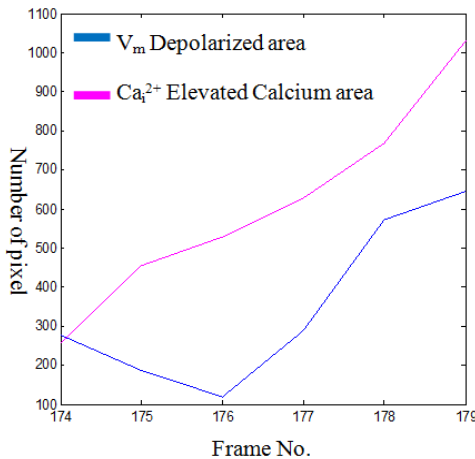Figure 9.   Focal point of new excitation wavefront of the Vm and Cai^{2+}

Figure 10. The number of pixels indicated this excitation propagation of the Vm and Cai^{2+} meant the focal point of new excitation

IV.   DISCUSSION

Experiments to induce late phase 3 EAD related VF were conducted that simulated abnormal heart conditions by the application of isoproterenol and nicorandil. Simultaneous measurements of the V_m and Ca_i^{2+} were conducted after strong shock during VF. A phenomenon implying that VF was likely induced by late phase 3 EAD was observed in one episode. The phenomenon observed might be late phase 3 EAD, and this is supported by the following findings:

1) There was large calcium transient in the 1st postshock activity, as shown in Fig. 11. The shortening of

APD was also observed for the 2nd postshock activity. These two conditions are considered to be essential for inducing late phase 3 EAD [8].

2) As is illustrated in Fig. 11, the activation timing of the Ca_i^{2+} was earlier than the upstroke of the V_m. This finding was confirmed from the waveforms as well as from an analysis of the size of the depolarized area and elevated calcium area, respectively, for the image frames 174 to 179 during the 3rd postshock activity (Fig. 9). In addition, the Ca_i^{2+} remained elevated after the VF restarted, consistent with the findings of previous studies [8].

3) The analysis of the size of the elevated calcium region and depolarized area revealed that these areas gradually expanded from the focal point (that regarded as the location where late phase 3 EAD occurred) of the new excitation (Fig. 10).

It is necessary to mention that the focal excitation propagation that was suggested could be from the reverse side of the heart, which should be the case. Future studies using 3-D optical mapping of the heart would be necessary to clarify this possibility. The experimental data clearly showed features such as a long Ca_i^{2+} transient and short APD, conditions that can lead to late phase 3 EAD.
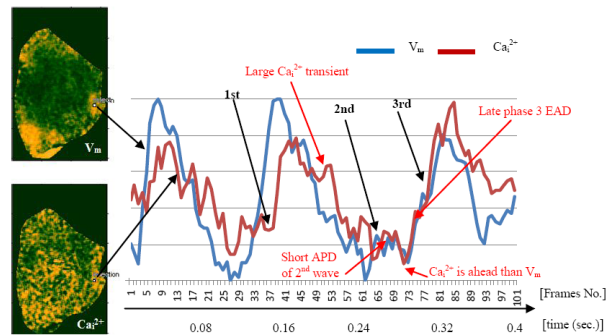

Figure 11. The proof features of late phase 3 EAD

On the other hand, the induction of late phase 3 EAD was a challenging task, because it is a difficult phenomenon to induce, and originally it is considered to be occurred on HF or ischemia heart, along with several factors need to be considered, such as: the experimental conditions (e.g. the rabbit heart model (in order to induce late phase 3 EAD, several trials using different concentrations of infused isoproterenol and nicorandil were performed in the Langendorff-perfused rabbit heart)), experimental equipment and protocol.

In addition, because the calcium map was noisy, observation of the excitation of the heart was complicated. This could have been caused by several factors, such as the elapsed time of the dual optical mapping of the V_m and Ca_i^{2+} (before the perfusion condition deteriorates). Also, the LED ring light intensity was not strong enough to obtain high quality signals.

The late phase 3 EAD reported in previous studies was obtained for the basal portion of the RV of the HF rabbit by means of an optical mapping system with a temporal resolution of 2ms and spatial resolution of 100×100 pixels ($0.35mm \times 0.35mm$ per pixel) [8]. And the accuracy

of the registration was not reported then there were limited data for identification of the location where the late phase 3 EAD occurred in the previous study.

In our experimental settings, the temporal resolution was 4ms and the spatial resolution was 512×512 pixels ($0.09mm \times 0.09mm$ per pixel). Although 5×5 spatial averaging was used to obtain the Ca_i^{2+} maps in the data analysis, the individual waveforms at each pixel could be analyzed. Thus, it is considered that our simultaneous V_m and Ca_i^{2+} optical mapping system has superiority to the previous measurement system, despite the lower temporal resolution.

Although data corresponding to the possible late phase 3 EAD phenomena were noisy, propagation of the depolarization of the membrane potential and the elevation of calcium could be analyzed. The location where the late phase 3 EAD may have occurred and led to subsequent VF was identified.

This was only possible by the introduction of an accurate image registration method for V_m and Ca_i^{2+} optical mapping data. Using the more accurate registration in the alignment process of the V_m and Ca_i^{2+} images resulted in the localization of the area where late phase 3 EAD likely was originated, and which led to the subsequent restarting of the VF.

In other words, by means of our optical system with high spatial resolution and an accurate alignment registration of the V_m and Ca_i^{2+} images, an accurate analysis and identification of the area where the late phase 3 EAD arose was achieved.

The results shown in the previous section are therefore considered to provide the first clear objective data that shows that VF may have initiated from late phase 3 EAD.

A certain limitation is that the present study comprised one experimental episode showed that VF was likely to be initiated from late phase 3 EAD. Therefore, the results should be confirmed in a larger number of experimental episodes. However, this analysis will contribute to detailed exploration of complicated cardiac electrophysiological phenomenon.

V. Conclusions

Measurements of postshock activities after electric shock during VF in a pathological model using an isolated rabbit heart specimen were conducted to gain an understanding of the mechanism underlying late phase 3 EAD and the origin of the subsequent VF arising due to late phase 3 EAD.

The analysis of late phase 3 EAD using the optical mapping system reported in this study may be the first stage toward understanding the location of this complex phenomenon that may require particular conditions.

These findings can be only obtained by the introduction of a V_m and Ca_i^{2+} simultaneous optical mapping system with high spatial resolution and accurate image registration (spatial resolution $0.48mm \times 0.48$ mm, registration accuracy of less than 2 pixels).

Furthermore, reporting a new type of analysis and findings on the mechanism underlying late phase 3 EAD and the origin of the subsequent VF due to late phase 3

EAD will be helpful for future studies in order to determine the optimal area for ablation that is precisely where cardiac arrhythmia occurs.

References

[1] C. F. B. van Huls van Taxis, A. P. Wijnmaalen, *et al.*, "Reversed polarity of bipolar electrograms for predicting a successful ablation site in focal idiopathic right ventricular outflow tract arrhythmias," *Heart Rhythm*, vol. 8, pp. 665-671, May 2011.

[2] Y. J. Chen, S. A. Chen, Y. C. Chen, *et al.*, "Effects of rapid atrial pacing on the arrhythmogenic activity of single cardiomyocytes from pulmonary veins: Implication in initiation of atrial fibrillation," *Circulation*, vol. 104, pp. 2849-2854, September 2001.

[3] A. Burashnikov, C. Antzelevitch, "Reinduction of atrial fibrillation immediately after termination of the arrhythmia is mediated by late phase 3 early afterdepolarization-induced triggered activity," *Circulation*, vol. 107, pp. 2355-2360, February 2003.

[4] M. Haïssaguerre, P. Jaïs, D. C. Shah, *et al.*, "Spontaneous initiation of atrial fibrillation by ectopic beats originating in the pulmonary veins," *N Engl J Med.*, vol. 339, pp. 659-666, September 1998.

[5] A. Burashnikov and C. Antzelevitch, "Late-phase 3 EAD. A unique mechanism contributing to initiation of atrial fibrillation," *Pacing Clin Electrophysioly*, vol. 29, pp. 290-295, March 2006.

[6] B. G. Katzung and J. A. Morgenstern, "Effects of extracellular potassium on ventricular automaticity and evidence for a pacemaker current in mammalian ventricular myocardium," *Circulation research*, vol. 40, pp. 105-111, January 1977.

[7] C. A. Martin, G. D. K. Matthews, and C. L. H. Huang, "Sudden cardiac death and inherited channelopathy: The basic electrophysiology of the myocyte and myocardium in ion channel disease," *Heart BMJ Journals*, vol. 98, pp.536-543, October 2011.

[8] S. K. Chua, P. C. Chang, M. Maruyama, I. Turker, T. Shinohara, M. J. Shen, Z. Chen, *et al.*, "Small-conductance calcium-activated potassium channel and recurrent ventricular fibrillation in failing rabbit ventricles," *Circulation Research*, vol. 108, pp. 971-979, April 2011.

[9] I. Hernandez, T. Arafune, N. Shibata, *et al.*, "Image registration for simultaneous membrane potential and calcium intracellular in rabbit hearts," *Journal of Transactions of the Japanese Society for Medical and Biological Engineering*, vol. 49, pp. 815-828, 2011.

[10] H. Hayashi, "Intracellular calcium dynamics and ventricular fibrillation," *Jpn. J. Electrocardioly*, vol. 29, pp. 219-225, June 2009.

Ignacio HERNANDEZ received a Ph.D. in Engineering from The University of Tokyo in 2012. He is currently a Research fellow in the Medicine School, Universidad Autónoma de San Luis Potosí México.
His research interests are in the areas of Rehabilitation, Biomedical Instrumentation, Functional Electrical Stimulation, Cardiac electrophysiology, Cardiovascular Physiology.

Tatsuhiko Arafune received a Ph.D. in Science from The University of Tokyo in 2004. He is presently Assistant Professor at School of science and Engineering, Tokyo Denki University.
His research interests are optical measurement, cardiac electrophysiology, image processing, spiral reentry analysis. He is a member of Japanese Society for Medical and Biological Engineering, Japan Society of Computer Aided Surgery and The Japanese Society of Electrocardiology.

Nitaro Shibata received a Ph.D. in medicine from Tokyo Womens Medical University in 1982. His present position is President of Shinjuku Mitsui Building Clinic.
His research interests are cardiac electrophysiology, biomedical signal analysis, medical pharmacology, and social medicine. He is a member of Japanese Biomedical Engineering Society, Japanese Circulation Society.

Masatoshi Yamazaki received a Ph.D. from Nagoya University, Graduate School of Medicine in 2006. His present position is Assistant

Professor at Research Institute of Environmental Medicine (RIEM), Nagoya University.

His research interests include basic and clinical cardiac electrophysiology. He is a member of Heart Rhythm Society, Japanese Heart Rhythm Society, Japanese Circulation Society and The Japanese Society of Internal Medicine.

Haruo Honjo, Ph.D., graduated from Nagoya University, Graduate School of Medicine in 1989. He became Associate Professor (1999-present) at Research Institute of Environmental Medicine Division of Stress Adaptation and Protection.

His current Research Fields are: Circulatory organs internal medicine, Cellular Physiology, Cardiac electrophysiology, Arrhythmia.

He is a member of The Japanese Society of Electrocardiology, The Japanese Circulation Society, Japanese Society for Medical and Biological Engineering, others.

Ichiro Sakuma received a Ph.D. in Engineering from The University of Tokyo in 1989. He is presently professor at School of Engineering, The University of Tokyo.

His research interests are biomedical engineering, computer aided surgery. He is a member of Japanese Society for Medical and Biological Engineering, Japan Society of Computer Aided Surgery and The Japan Society for Precision Engineering.